NASA/TM—1998-112231
USAATCOM-TR-98-A-004

Flight-Time Identification of a UH-60A Helicopter and Slung Load

Luigi S. Cicolani
Ames Research Center, Moffett Field, California

Allen H. McCoy
U.S. Navy Post Graduate School
Monterey, California

Mark B. Tischler
Aeroflightdynamics Directorate
U.S. Army Aviation and Troop Command
Ames Research Center, Moffett Field, California

George E. Tucker
Ames Research Center, Moffett Field, California

Pinhas Gatenio and Dani Marmar
Israel AF Flight Test Center, Instrumentation Department, Israel

National Aeronautics and
Space Administration

Ames Research Center
Moffett Field, California 94035-1000

April 1998

Acknowledgments

Many individuals made significant contributions to the conduct of these flight tests, including the Ames test pilots (Ricky Simmons, Ltc Chris Sullivan, Munroe Dearing) and crew chief (Jim Phillips), the aircraft support crew and load handlers (Leonard Hee, John Lewis, Perry Silva, Paul Everhard), the telemetry support group (Sun-Yat Ng, Mei Wei, Austin Somes, Mitch Aoyagi, Pam Phol), and the engineering and test services groups (Dave Groepler, Roy Williams, Chris Chen), and many others.

Available from:

NASA Center for AeroSpace Information
7121 Standard Drive
Hanover, MD 21076-1320
(301) 621-0390

National Technical Information Service
5285 Port Royal Road
Springfield, VA 22161
(703) 487-4650

Abstract

This paper describes a flight test demonstration of a system for identification of the stability and handling qualities parameters of a helicopter-slung load configuration simultaneously with flight testing, and the results obtained. Tests were conducted with a UH-60A Black Hawk at speeds from hover to 80kts. The principal test load was an instrumented 8x6x6ft cargo container. The identification used frequency domain analysis in the frequency range to 2Hz, and focussed on the longitudinal and lateral control axes since these are the axes most affected by the load pendulum modes in the frequency range of interest for handling qualities. Results were computed for stability margins, handling qualities parameters and load pendulum stability. The computations took an average of 4 minutes before clearing the aircraft to the next test point. Important reductions in handling qualities were computed in some cases, depending on control axis and load-sling combination. A database, including load dynamics measurements, was accumulated for subsequent simulation development and validation.

1. Introduction

Helicopter slung load operations are common in both military and civil contexts. The slung load adds load rigid body modes, sling stretching, and load aerodynamics to the system dynamics, which can degrade system stability and handling qualities and reduce the operating envelope of the combined system below that of the helicopter alone.

Military helicopters and loads are often qualified for these operations via flight tests which can be expensive and time consuming. These activities include certification of loads for the multi-service Helicopter External Air Transport (HEAT) manual (ref. 1), in which pilots evaluate specific load-helicopter combinations for flying qualities and airspeed limits without analytical support and without generating quantitative stability data. There can also be extended tests, including analyses, to certify a helicopter load carrying capacity, (ref. 2). However, stability and envelope can vary significantly among the large range of loads, slings, and flight conditions which a utility helicopter will encounter in its operating life, and flight tests cannot practicably encompass the entire operating range of configurations.

A recent industry paper (ref. 2) has advocated the accumulation of quantitative stability data from slung load certification flight tests and pointed out the potentially significant reductions in cost and risk available from using a validated simulation to predict stability for a variety of sling-load combinations and to predict the critical cases for flight test evaluation. Towards these objectives, an exploratory project was initiated at Ames in which flight tests were conducted to demonstrate identification of aircraft stability and handling qualities and load pendulum stability simultaneously with the flight test. Such a capability would have potential for significant reductions of qualification tests in comparison to point-by-point testing. Stability evaluations were made after each test airspeed before going on to the next. A database was also accumulated for subsequent simulation development and validation efforts.

This paper describes the flight test method and results. The test aircraft was a UH-60A Black Hawk, and the principal test load was an instrumented 8x6x6 ft CONEX cargo container. The CONEX is a low-density load with significant aerodynamics such that load stability limits the system flight envelope. The load instrumentation included accelerometers, angular rate sensors, and fluxgate compass, and was provided by the Israel Flight Test Center under a US/Israel memorandum of agreement for cooperative research on rotorcraft aeromechanics and man-machine integration technology (ref. 3). Under this agreement the US would provide the aircraft, load, and test range and Israel would provide an instrumentation package and wind tunnel testing. The load instrumentation allowed

computation of load stability parameters during flight tests, and documented details of the load dynamics not previously available for simulation validation.

Tests focused on the longitudinal and lateral axes in which the load pendulum motions have their principal effects on aircraft control. Tests were conducted at airspeeds between hover and 70kts. The identification computations used the CIFER® software previously developed by the Army group at Ames (refs. 4 and 5).

The paper begins with a discussion of the parameters to be identified and the required computations for that, followed by descriptions of the test configurations, the test instrumentation, the flight test profile, and the data acquisition system and computational procedure for flight time identification. Identification results for all parameters are presented. The paper ends with a brief comparison of load motions from flight and simulation, and an assessment of simulation development issues. Reference 6 provides more extensive documentation of the test equipment and results.

2. Identification Computations

2.1 Dynamic System

The dynamic system (fig. 2.1) consists of helicopter and load. A stability augmentation system is closed around this, and the pilot closes another loop around that combination to regulate the system to a desired flight path. The plant element is rich in dynamics which include the helicopter's rigid body modes, rotor modes, engine and drive train modes, and structural modes; and the load adds its rigid body and elastic sling modes to this set.

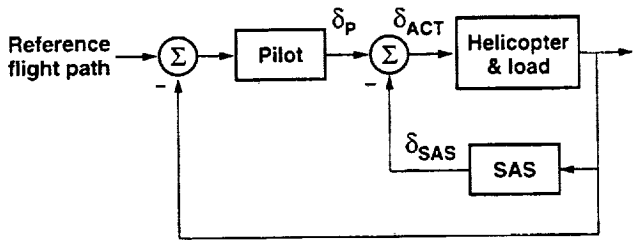

Figure 2.1 Dynamic System.

Over the years, the US military has developed handling qualities requirements that the closed loop system must meet to avoid PIO tendencies when the pilot exercises control (ref. 7), and stability margins that the stability augmentation system (SAS) must meet to avoid potentially destructive resonance with the plant dynamics (ref. 8). The clearance of loads is concerned with evaluating these handling qualities and stability margins for the combined system and the stable speed envelope of the load. Quantitative assessment of stability and handling qualities is based on frequency domain analysis of the dynamic system.

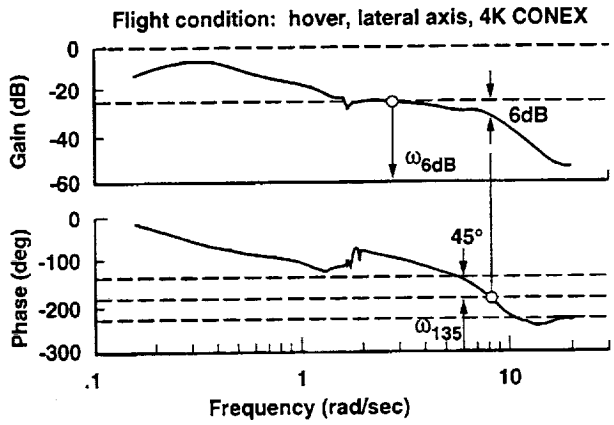

Bandwidth: $\omega_{BW} = \min\{\omega_{6dB}, \omega_{135}\}$

Phase delay: $\tau_{PD} = -\frac{\Phi(2\omega_{180}) + 180}{2\omega_{180}}$ or $-\frac{1}{2}\left(\frac{d\Phi}{d\omega}\right)_{\Phi = 180}$

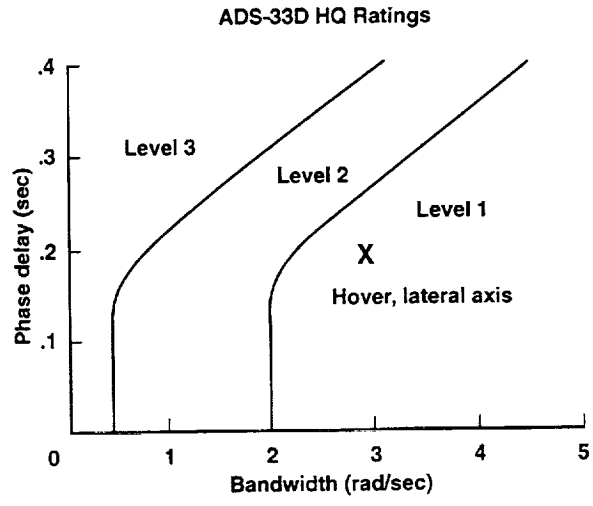

Figure 2.2. Handling Qualities Parameters from Attitude Response.

2.2 Handling Qualities

The handling qualities parameters are properties of the closed loop attitude frequency response. Two primary parameters are bandwidth and phase delay (fig. 2.2). Bandwidth is measured as the maximum input frequency for which 6db of gain margin and 45 deg of phase margin can be obtained. Figure 2.2 indicates the required computations are to determine the two frequencies where these margins are obtained and then bandwidth is taken as the smaller of the two. Instances occur in which phase is below -135 deg at all frequencies, in which case bandwidth is zero. Phase delay is the rate at which phase changes at the frequency where the phase shift is 180 deg, and can be computed from a two-point estimate or a least squares fit at that frequency.

Phase delay indicates how rapidly the system is going unstable as the input frequency approaches the point of 180 deg phase shift. Larger values imply a rapid loss of pilot-vehicle stability margins, and result in pilot complaints about PIO tendencies.

Army specifications for these parameters are defined in an Aeronautical Design Standard document, ADS-33D (ref. 7). A satisfactory system is required to have its combination of bandwidth and phase delay within a specified region, termed level 1, where simulation and flight tests indicate satisfactory pilot ratings are obtained (fig. 2.2). Additional regions are level 2 (satisfactory with improvements) and level 3 (unsatisfactory). At phase delays below .15 sec the specifications require a minimum bandwidth of 2rad/sec for level 1. For phase delays above .15 sec, increased phase delay requires more bandwidth.

The ADS-33D specifications for handling qualities were defined to serve the Comanche (RAH-66) procurement, with the object of providing acceptable behavior for a suite of tasks appropriate to scout attack rotorcraft. It includes requirements for other motion parameters in addition to the on-axis attitude response parameters computed in this study. ADS-33D is based on simulation data and flight data from several helicopters including the UH-60. Although slung load tasks were not included in the ADS-33D specification, the ADS-33D levels 1-3 will be used as the reference specifications for the present discussion. Another Army project at Ames is currently in progress to extend that specification to cover cargo helicopters and slung load operations in support of the improved cargo helicopter procurement (ref. 9).

2.3 Stability Margins

Stability margins define the stability robustness of the aircraft/SAS feedback loop to changes in gain (gain margin) and phase (phase margin). Typical requirements from MIL-F-9490D (ref. 8) are for 6db of gain margin (a factor of 2) and 45 deg of phase margin. These margins also ensure well-damped responses to turbulence and pilot inputs. The UH-60 has roll, pitch and yaw SAS channels, and stability margins can be computed for these channels.

The control system stability margins are properties of the control loop computed from the broken-loop frequency response of the SAS signal to the inputs to the primary actuators as shown in figure 2.3. The phase margin is computed at the crossover frequency where the gain crosses through 0db, and is the margin from 180 deg of phase shift there. There can be multiple crossings, as in the sample case, in which case the phase margin (PM) is taken as the smallest phase margin for crossings in the frequency range of interest [.05, 2.0]Hz. Cases occur in which gain never crosses below 0db, in which case phase margin is infinite and instability cannot occur. The gain margin (GM) is computed where the phase angle goes through 180 deg.

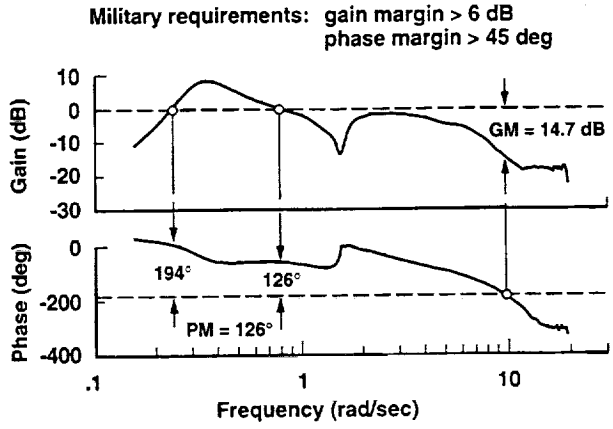

Figure 2.3. Stability margins from control response $\frac{\delta_{SAS}(s)}{\delta_{ACT}(s)}$

2.4 Load Pendulum Modes

Linear analysis indicates the load adds a number of modes to those of the helicopter alone; these are two pendulum modes, two yaw modes, and 3 oscillatory sling stretching modes. Of these, only the pendulum modes interact with the helicopter in the frequency range of interest. The pendulum frequencies can be estimated from a point mass dumbbell approximation of the system as

$$\omega_p = \sqrt{\frac{g}{\ell}\left(1+\frac{W2}{W1}\right)}$$

where ℓ, W1, W2 are sling length, and the helicopter and load weights, respectively. Pendulum frequencies of 1 to 1.5 rad/sec can be estimated for the current configurations.

Simulation model analysis indicates that the pendulum modes at hover are decoupled lateral and longitudinal pendulum motions relative to the helicopter and that these are readily excited by lateral and longitudinal control inputs, respectively. Consequently, each mode can be identified by fitting a second order pole to the frequency response of the load angular rate in the region around the pendulum frequency. A typical frequency response is shown in figure 2.4; gain peaks near the expected load pendulum frequency, and the fitted 2nd order system is seen to achieve a close fit to the flight data.

3. Flight Test Configurations

3.1 Test Configurations

Flight tests were performed with an instrumented UH-60A and with several test external loads and slings (fig. 3.1). It is noted that the UH-60 without a load has significant stability margins from the minimums allowed and is thus a safe aircraft for slung load research where margins can be reduced by the load. The load-sling combinations tested are drawn to scale in figure 3.2. These included an instrumented CONEX (CONtainer EXpress) cargo container, a steel plate, and a steel block suspended with single and multi-cable slings.

The plate and block were well-behaved out to the power-limited level flight speed of the aircraft (about 140 kts) and were used in the first phase of the work. The CONEX was an easily available load with nontrivial and complex aerodynamics which limit its operational envelope to 60 kts.

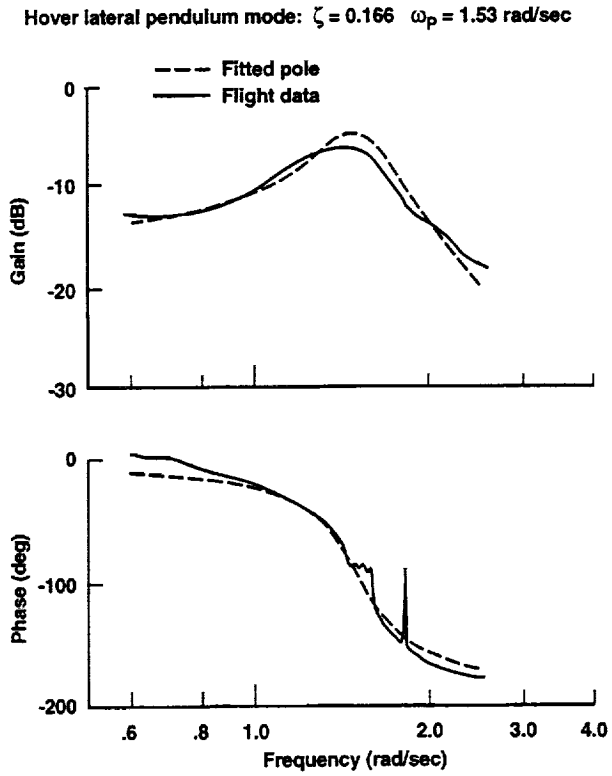

Figure 2.4. Identification of load pendulum roots.

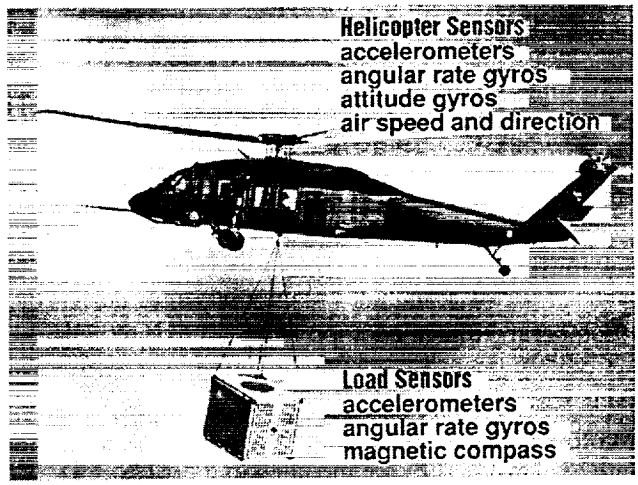

Figure 3.1. UH-60 with CONEX load.

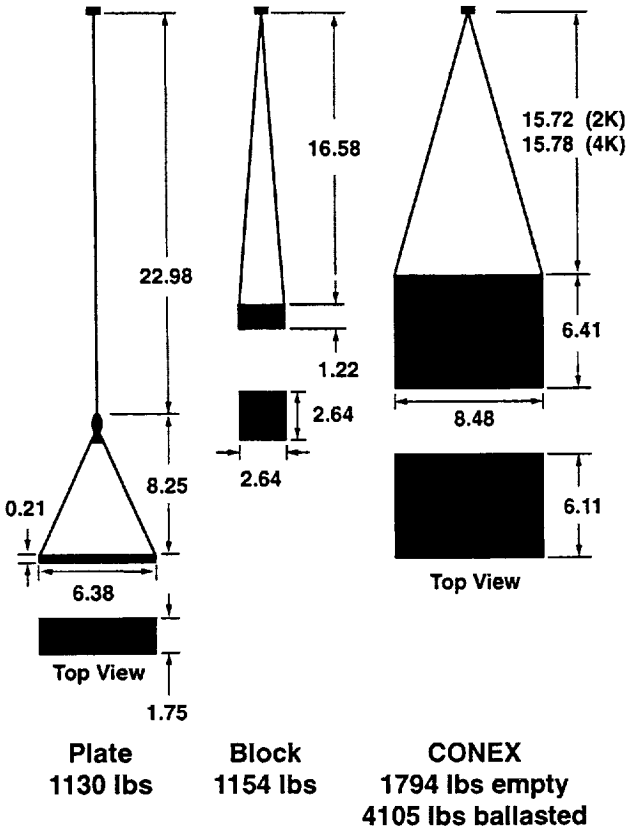

Figure 3.2. Load-sling test configurations.

Slung load configurations can be viewed as two rigid bodies connected by a sling. In general, the configuration can be defined by all the fixed parameters of the helicopter, the load, and the sling for which numerical values are required in the system's equations of motion. All of these parameters play some more or less important role in the motions of the 2-body system which can be studied in simulations. Out of the existing range of such systems, the present tests are limited to one helicopter, and a small sample of slings and loads, but this suffices for our immediate objectives.

3.2 Helicopter Parameters

The helicopter's basic rigid body parameters are listed in figure 3.3. The gross weight and cg location are standard takeoff values for this aircraft with slung load crew (2 pilots and crew chief). Approximately 1800 lbs of fuel (2 hrs of flight) is available for use during a test, with corresponding changes in gross weight and with forward movement of the cg by 9 in. Aerodynamic and other information for the UH-60 can be found in [10] - [13].

The UH-60A hook (fig. 3.4a) is mounted in the floor of the helicopter and can be released manually at the hook or from the right seat stick. It is gimbaled only in roll so that the load-sling combination swings laterally about this axis, and longitudinally at the hook load beam about 8in lower. The hook is offset 4.3ft below the aircraft cg and up to 1 ft forward of the cg depending on fuel weight, and is rated at 8000 lbs carrying capacity.

Figure 3.3 Helicopter and Load Rigid Body Parameters.

(a) Helicopter

Takeoff Weight	14,601 lbs.
Max External Load	8,000 lbs.

Coordinates	**Takeoff cg**	**Hook**
station	363.5	352.6 in
butt line	0	0
water	247.2	195.5 in

(b) Loads

Load	**Plate**	**Block**	**Empty CONEX**	**Ballasted CONEX**
Weight	1130	4154	1794	4105 lbs.
Density	456	488	5.4	12.5 lbs./ft^3
Ixx	108	91	785	1876 slg-ft^2
Iyy	212	91	569	1482
Izz	121	150	766	1377
Zcg	-.4	0	0	1.4 ft.

Notes:

- Inertias, Ixx, ..., are computed about the load cg.
- Axes used for inertias are:
  plate: x along the long dimension, z down
  block: x along a horizontal edge, z down
  CONEX: y along longest dimension, z down
- Zcg = vertical distance from geometric center to cg, positive down
- CONEX data includes installed instrumentation

3.3 Load-Sling Parameters

Flight test data was obtained for the aircraft alone and with the sling-load combinations shown in figure 3.2. Load weights ranged from 1000 lbs to 4000 lbs (up to 50% of the hook capacity and 28% of helicopter weight). The CONEX weight was varied by ballasting it with bags of gravel-like material of density 43 lbs / ft^3, and it was flown empty at about 2K lbs. and ballasted at 4K lbs.

The dimensions of these load-sling combinations are noted in figure 3.2, and mass-inertia data for these loads is listed in figure 3.3. Figure 3.2 gives an impression of the differences in sling length and geometry. These differences are moderate, but quite different results were obtained at hover among these loads, probably due to these geometric differences.

The 1K plate load consisted of a steel plate (1070 lbs.) and wire bridle with swivel and ring (60 lbs.). It was suspended with a standard 20ft military sling comprised of 2 loops of flat nylon webbing, and attached at the ends with nylon rings (fig. 3.4b). Such slings are described in reference 1 and occur in the US military inventory in various lengths from 3 to 140 ft.

The remaining test loads were suspended with a standard military 4-legged sling set rated at 10K lbs. and weighing 52 lbs. Each leg of this sling is a 12 ft braided nylon rope connected to an 8ft steel chain which is passed through a load lift point and returned to a grabhook at the end of the rope (fig. 3.4c). The details of rigging this sling to certified loads such as the CONEX, are specified in the HEAT manual (ref. 1). Similar sling sets with ratings up to 40K lbs. occur in the military inventory and can be rigged with 2 to 6 legs, depending on the load as seen in the HEAT manual, (ref. 1). This sling was flown in the present tests with and without a swivel, and the resulting load yaw motions at airspeed were quite different.

Sling stretch properties will not be discussed in detail since stretching occurs at frequencies well above the range of interest in handling qualities studies. The slings are fairly stiff and stretching was estimated at a fraction of 1 ft in all cases. The sling lengths given in figure 3.2 are for the loaded sling.

3.4 Load Aerodynamics

The available aerodynamic data for slung loads is limited to a few specific loads. Load aerodynamics are unimportant for very dense loads such as the steel plate and block loads (450 lbs / ft^3). These can be flown over the power-limited speed range of the helicopter without generating significant aerodynamic specific forces and moments. The CONEX is much less dense (5-12 lbs / ft^3 average density in the present tests) and can generate sufficient aerodynamics to affect load motions. The effects include a load trail angle in proportion to the drag specific force, and modification of the load pendulum motions in various ways as airspeeds increases, including coupling of the yaw degree of freedom with the load lateral and longitudinal pendulum motions and a speed limit for stability well below the helicopter's power–limited speed. The CONEX drag can be estimated at D/Q = 75 ft^2 which yields trail angles of 19.5 deg and 8.8 deg for the empty and ballasted CONEX at 50kts, respectively, and these loads reach .5g specific drag at 60, and 90kts, respectively.

The principal parameters affecting load motions are as follows. The load pendulum frequency is set principally by sling length and load relative weight, while helicopter cg-to-hook offset couples the load motions to the helicopter attitude dynamics which then are a source of damping in accordance with helicopter aerodynamics and inertias. Load aerodynamic forces and moments increase with airspeed and have an increasing effect on load dynamics depending on the magnitude of the specific forces and moments produced.

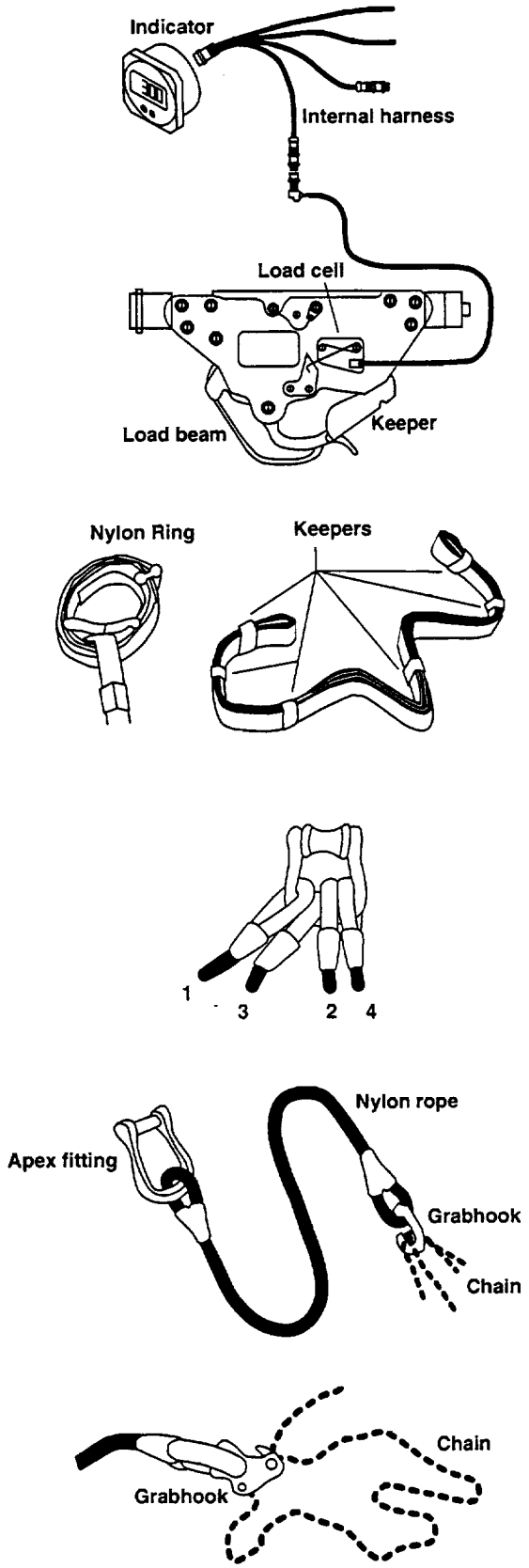

Figure 3.4. Suspension Details ([1], [17]).

4. Instrumentation and Signals

4.1 Helicopter and Load Sensors

The test aircraft was heavily instrumented for an earlier airloads study at Ames, as described in (ref. 14). The sensors recorded for the slung load tests were those measuring the aircraft rigid body states and control deflections. These are listed in figure 4.1 along with sensor ranges and the data sampling rates for recording and telemetry (209 HZ). The hook was also instrumented with a strain gauge load weight cell (ref. 15).

The load instrumentation is listed in figure 4.1. This included a gimballed magnetic fluxgate compass (ref. 16) mounted on an aluminum boom extending 2.5ft from the CONEX (fig. 4.2) to minimize magnetic interference from the steel CONEX. The remaining load instrumentation (ref. 17) was contained in a single package mounted on an aluminum crossbeam installed in the CONEX near the geometric center (fig. 4.2). The instrumentation package (fig. 4.3) contained 3-axis accelerometers and angular rate sensors, and also pitch and roll inclinometers. This package, including power supply, filters, PCM encoder, and telemetry transmitter was assembled at an estimated cost of $40K, and weighed 119 lbs. including the mounting.

Figure 4.1 Instrumentation

Helicopter sensors sample rate = 209 Hz	**Range**	**Load sensors** sample rate = 260 Hz	**Range**
Longitudinal stick position	[0, 100] %	Roll Inclinometer	[-90, 90] deg
Lateral stick position	[0, 100] %	Pitch inclinometer	[-90, 90] deg
Pedals	[0, 100] %	Fluxgate compass	[0, 360] deg
Collective	[0, 100] %	Roll rate gyro	[-60, 60] deg/sec
Longitudinal SAS output	[0, 100] %	Pitch rate gyro	[-60, 60] deg/sec
Lateral SAS output	[0, 100] %	Yaw rate gyro	[-120, 120] deg/sec
Directional SAS output	[0, 100]%	Longitudinal accelerometer	[-2, 2] g
Longitudinal mixer input	[0, 100] %	Lateral accelerometer	[-2, 2] g
Lateral mixer input	[0, 100] %	Vertical accelerometer	[-1, 3] g
Directional mixer input	[0, 100] %		
Roll angle	[-90, 90] deg		
Pitch angle	[-90, 90] deg		
Directional gyro	[0, 360] deg		
Roll rate gyro	[-50, 50] deg/sec		
Pitch rate gyro	[-50, 50] deg/sec		
Yaw rate gyro	[-50, 50] deg/sec		
Longitudinal accelerometer	[-2, 2] g		
Lateral accelerometer	[-2, 2] g		
Vertical accelerometer	[-2, 4] g		
Angle-of-attack vane	[-100, 100] deg		
Sideslip vane	[-100, 100] deg		
Dynamic pressure	[0, 2] in. Hg		
Static pressure	[20, 32] in. Hg		
Stagnation temperature	[-20, 50] deg C		
Longitudinal low airspeed	[-35, 165] kts		
Radar altimeter	[0, 1,500] ft		
Hook load	[0 10,000] lbs.		

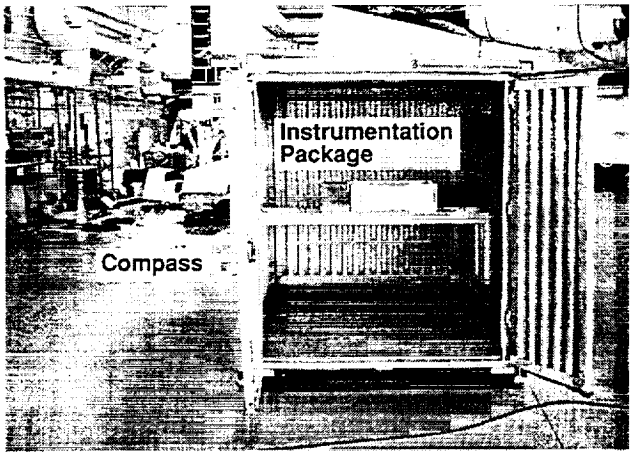

Figure 4.2. CONEX Instrumentation

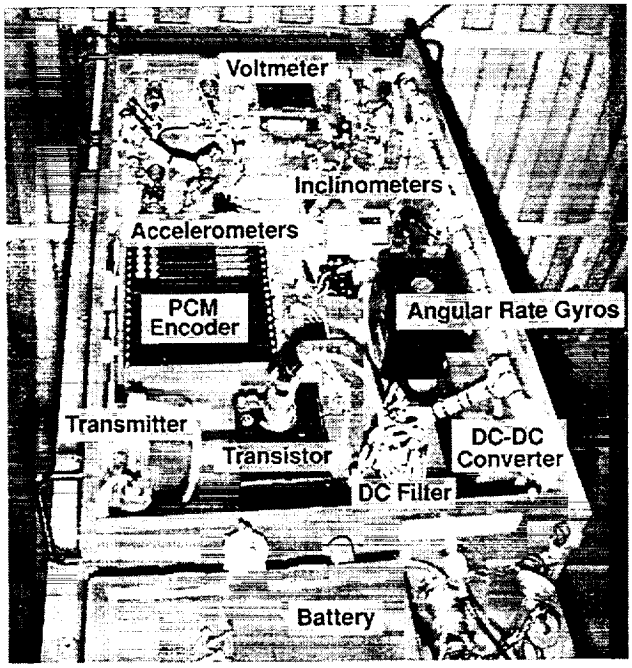

Figure 4.3. CONEX Instrumentation Package

4.2 Overview of Sensors

This sensor set is more than is needed for the identification computations, which require only the helicopter and load angular rates and heading, and the control positions. The set is somewhat short of measuring all the rigid body states of the two bodies and the forces and moments at the hook; and short of what's needed to measure the load aerodynamics. Omitted states and variables include load velocity vector and the hook force direction angles. Further, the inclinometers and hook load cell are devices designed for static conditions and were subject to significant uncorrectable errors under dynamic pendulum motions, so that variations in load pitch and roll angles and hook force magnitude were not adequately sensed.

The load dynamic range was larger than anticipated in yaw, where yaw rates above 100 deg/sec occurred for airspeeds above 50kts. This resulted in saturation of the load yaw rate gyro 120 deg/sec limit and corresponding large dynamic lags in the fluxgate compass at the higher test airspeeds.

The present load sensors provide good access to the pendulum dynamics up to 50kts airspeed and limited access to the load aerodynamics for the simulation validation effort.

4.3 Signals

The helicopter sensors are standard types whose signal properties are already familiar in the flight test literature. The sensors of principal interest are the rate and heading gyros. The helicopter angular velocity signals from a typical frequency sweep (fig. 4.4) contain a moderate amount of vibration at 2-3 deg/sec amplitude and frequencies of 1-4 per revolution, plus biases up to 6deg/sec. Vibrations are well above and biases are well below the frequency range of the identification computations and have no effect on the results. The directional gyro was not slaved and had a random startup bias as well as a drift which required calibration at the start and end of each flight.

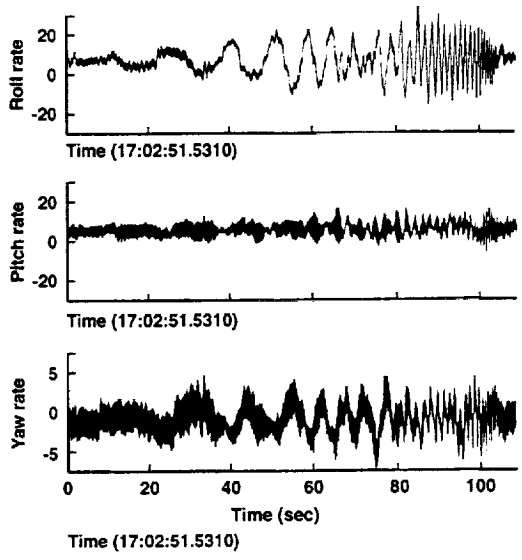

Figure 4.4. Helicopter rate gyro signals (deg/sec) 30kts, lateral sweep, flight 172, record 26.

The load accelerometer signals (fig. 4.5) don't contain the vibrations that dominate the helicopter accelerometer signals. The vertical accelerometer signal contains the centrifugal acceleration of the load pendulum swinging. This is visible during the time interval 60 to 80 secs when the pendulum mode is excited. The low frequency variations in the x, y accelerometers in this record (taken at 30 kts) are the signature of the steady load trail angle due to load drag combined with yaw motions which distribute the specific drag to the x and y accelerometers according to the yaw time history. It turns out that the pendulum swinging motions are not detectable by the x-y accelerometers because the apparent gravity associated with pendulum swinging is always close to the load vertical axis and along the sensitive axis of the vertical accelerometer.

The load angular velocity signals in figure 4.5 are free of high frequency content or noise to the resolution of the plot. The yaw history in this record indicates periodic yawing of the load by 80deg. The pitch and roll rate histories represent the angular velocity associated with load lateral pendulum motions which is distributed to the load pitch and roll rate sensors according to the load yaw history.

The fluxgate compass was subject to several systematic and dynamic errors. These included (1) transients at each crossing of the limits of its range at 0 and 360deg, (2) geometric errors due to misalignment from the true vertical during pendulum motions, and (3) large dynamic lags for load yaw rates above 90 deg/sec. The first of these was correctable. Correction of the second error requires measurement of the load pitch and roll attitude. However, analysis indicated the geometric error was moderately small in size for the load pendulum motions of the test, and could be ignored in the identification computations.

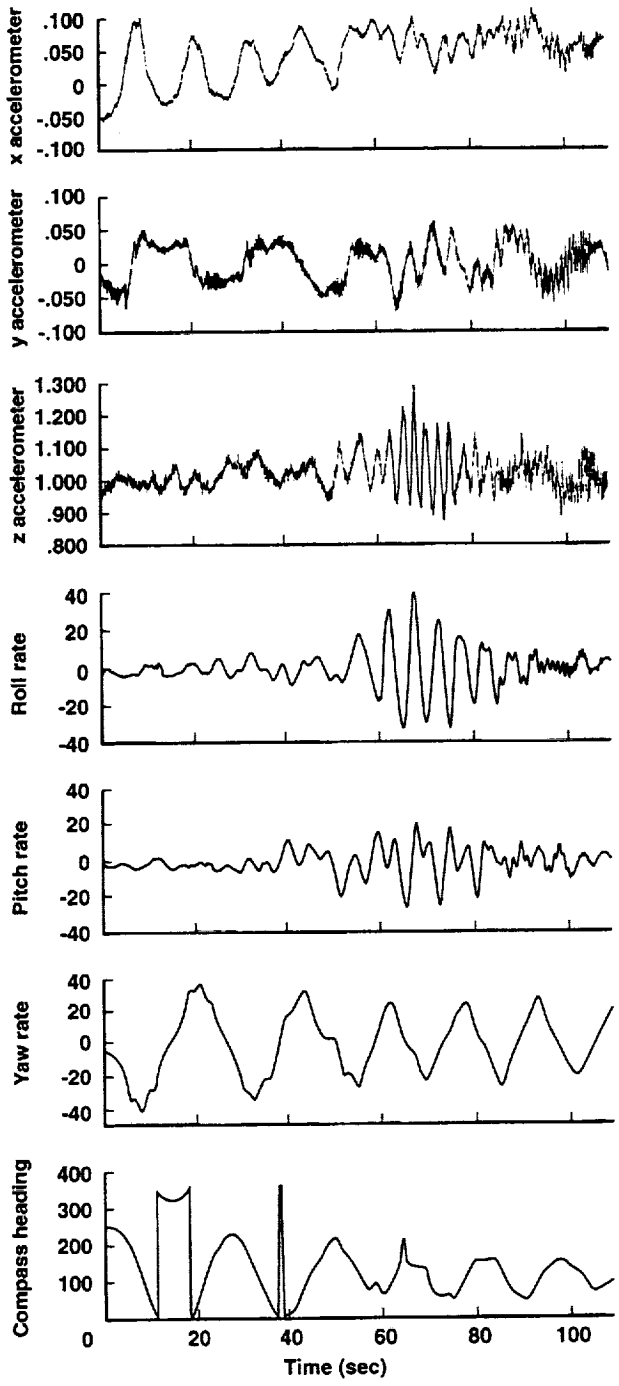

Figure 4.5. Load sensor signals (g, deg/sec, deg). Flight 172, record 26: 30 kts, lateral sweep, 4k CONEX.

4.4 Signal Processing

Relatively little processing of the received signals was required for the identification computations. The helicopter stability margins and handling qualities parameters could be computed almost

directly from the helicopter control and angular velocity signals.

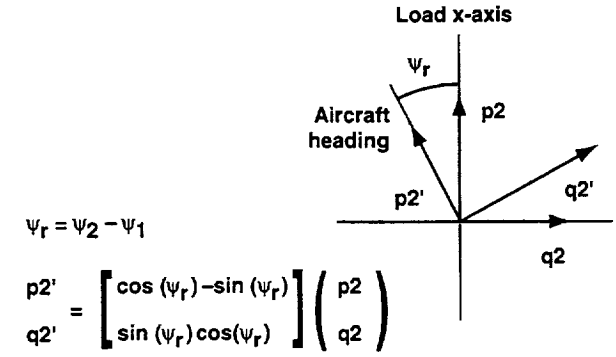

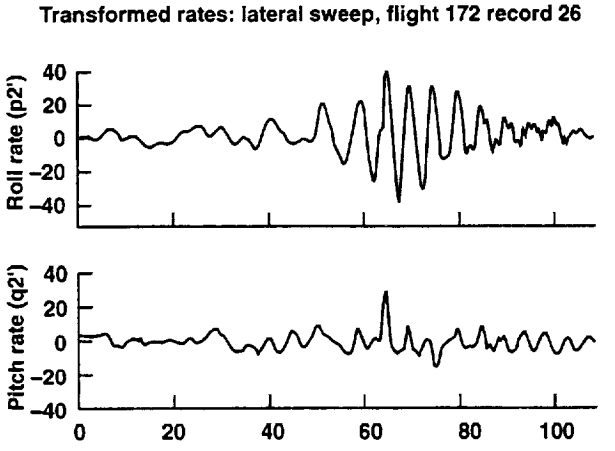

Figure 4.6. Transformed load angle rates.

Computation of load stability parameters required transformation of the load pitch and roll rate signals to axes aligned with the helicopter heading (fig. 4.6) to get sufficient correlation of the load angular rates with the control inputs for identification of the load pendulum roots. This was required because the load underwent arbitrary yawing which distributed the angular rates due to pendulum swinging to the pitch and roll rate gyros according to the yaw time history. The transformed signals for the lateral sweep record shown in figure 4.5 is included in figure 4.6, and shows that the load angular rates resolve principally into roll rotation about the helicopter longitudinal axis.

5. Flight Test Profile

5.1 Take-off Procedure

Flight tests were preceded by a briefing of the test team, including the aircrew, load handlers, telemetry staff and test engineers, to review test procedures, test points, load hook-up procedures and safety considerations.

Subsequently, the aircraft was powered up on the ramp and control calibrations were performed along with telemetry communications checks with the ground station, and directional gyro calibration. The load handlers waited near the load and, for the CONEX, powered up the load instrumentation and secured the doors.

The plate and block loads were hooked up with the aircraft on the ground. For the CONEX, the aircraft approached, stabilized over the load, and lowered to the desired height with guidance from the crew chief who was prone on the deck with a view through the hook hatch. Two load handlers stood on top of the CONEX, one to ground the hook and a second to lift the sling shackle onto the cargo hook (fig. 5.1). The rotor downwash carried a significant amount of airborne debris and buffeted the load handlers as the helicopter approached, but this lessened considerably with the helicopter directly overhead. After hookup, the handlers dismounted the load with the help of a handhold that was welded onto the CONEX near the top. Generally, the load hook-up procedures and equipment specified in the HEAT manual (ref. 1) were used.

5.2 Test Records

The flight data was taken with the stability augmentation system (SAS) on and the flight path stabilization system (FPS) off. The FPS would otherwise superpose control inputs on that of the pilot.

Flight test inputs at each flight condition usually consisted of a trim record, followed by 3 repeated frequency sweep records, and ending with pairs of steps and doublets in opposite directions. The identification computations used only the frequency sweep records and the remaining records were used for independent checks. This sequence was

performed principally with the longitudinal and lateral controls and at speeds of hover, 30kts, 50kts along with some data at higher speeds. A total of 11 data flights (11.5 flight hours) were performed during 1996–97 at Moffett Field with calm winds. A detailed listing of flights, loads, and data records is given in reference 6.

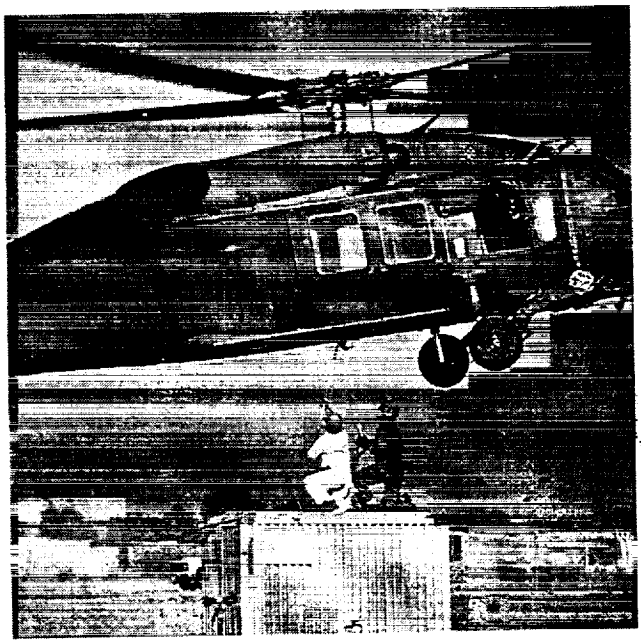

Figure 5.1. CONEX Hookup

5.3 Frequency Sweep Records

Identification based on frequency sweep flight test data has been developed over the past decade, and numerous examples have been reported in the literature. The design and execution of pilot-generated frequency sweep inputs has been considered in detail in references 18 and 19. The main considerations in generating good data are to remain generally centered about the reference trim flight condition; and to avoid large correlated secondary control inputs, gust disturbances, and excessive excitation of lightly damped modes in the frequency range of the test. Each aircraft and test frequency range have their own unique considerations, but the UH-60 at frequencies to 2Hz presented no special problems.

A sample lateral axis control sweep is shown in figure 5.2. The pilot begins with a short period of trim, then starts with two cycles at the minimum frequency (20sec period in this case), and increases frequency smoothly to 2 Hz, with the assistance of the copilot who calls out quarter cycles for the first two cycles and every 15secs thereafter. The test monitor indicates when 2 Hz has been reached and the complete sweep record is about 90secs long. The frequency range from .05 to 2 Hz is considered appropriate for handling qualities studies. The minimum value avoids large aircraft motions that can result from low frequency inputs and pilot input amplitude is reduced in this range as seen in figure 5.2, and otherwise amplitude is selected to maintain linearity. The maximum frequency is low enough to avoid resonance with the lowest structural and rotor modes. The load pendulum modes of interest in this study are well within this range at .25Hz.

The off-axis controls departed very little from their trim values, although there is a small amount of correlated pedal input. In general, correlated secondary control inputs reduce data quality, and the pilot tries to maintain the reference conditions with occasional uncorrelated low frequency off-axis inputs.

In figure 5.2, the helicopter roll rate response is held to about 10deg/sec maximum amplitude, and the (transformed) load roll rate is seen to have its principal response around resonance with the predicted pendulum frequency and with peak amplitude of 20deg/sec. The helicopter roll angle has its largest response at low frequencies and reaches 10deg. The reference pitch attitude and airspeed are well maintained in this sample. Generally, airspeed variations up to 10 kts around the reference speed can be tolerated without significant loss of linearity, and excursions of that size were common.

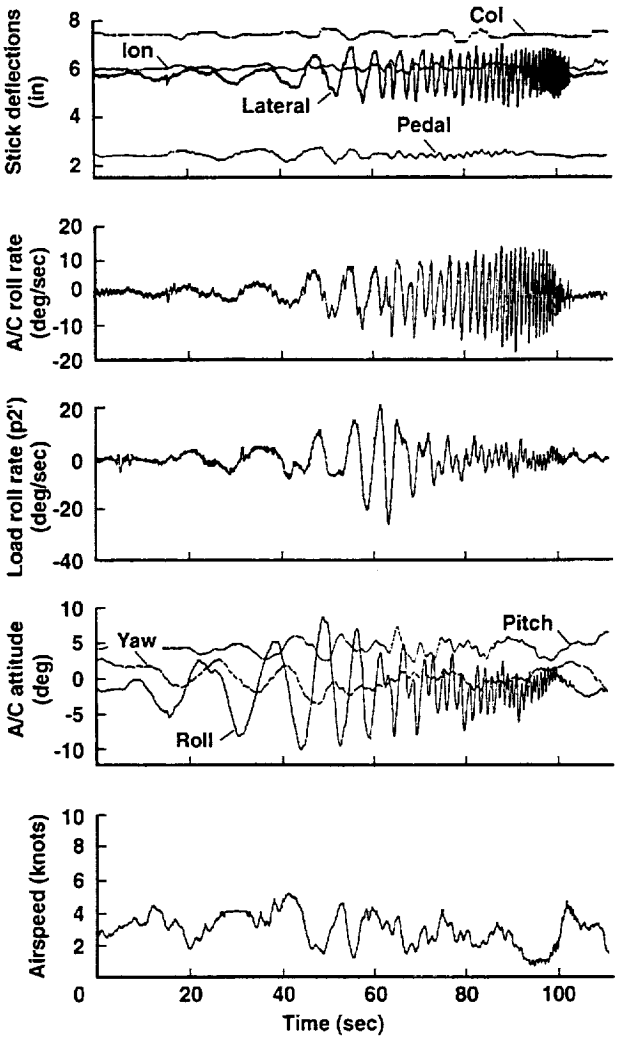

Figure 5.2. Sample lateral frequency sweep.
Flight 172, record 12: hover, 4k CONEX

6. Data Acquistion and Identification Procedure

6.1 Data Acquisition

The data acquisition system is shown in figure 6.1. All sensor signals were recorded on board the aircraft and telemetered simultaneously to the ground station, which was equipped for real time strip chart displays, data recording, and video monitoring of the aircraft when it was within range of the ground station cameras. The ground station and telemetry support was provided by the Western Aeronautical Test Range facility at Moffett Field.

A camera was also mounted in the aircraft looking down through the hook hatch at the load. This was successfully recorded on board but reception of the load video at the ground station was always poor. This video provided a visual record of load motions relative to the aircraft to augment the time histories from the instrumentation.

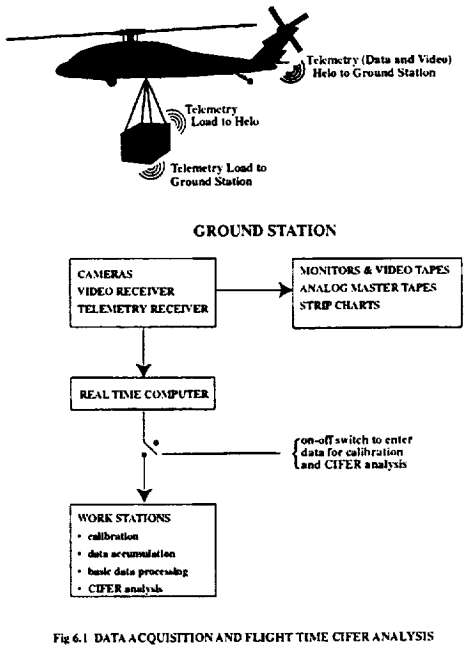

Figure 6.1. Data Acquisition and flight time CIFER analysis.

6.2 Flight Time Identification System

The flight time computations used a system of three workstations and required complex data communications across several networks from the real time telemetry receivers to the workstations. The system was implemented by the telemetry support group (ref. 20).

Data was input to the workstations using an on-off switch which allowed the test engineer to store and concatenate the three frequency sweep records obtained at each test condition. The required computations were then carried out using the CIFER® software (refs. 3 and 4) for interactive frequency domain analysis. This software has received wide application in the past decade to both helicopters and fixed wing aircraft, including instances of flight time identification (ref. 21). The CIFER® computations took an average of 4 minutes to perform. The workstations also contained logic to carry out and store the required initial calibration of the helicopter heading gyro and to process the

controls and load signals prior to the CIFER® computations.

6.3 Identification Procedure

The frequency domain identification procedure determines the frequency response functions between given input and output flight records. When the plant dynamics are nonlinear this produces a frequency response that best represents the first harmonic approximation of the dynamics. The residual signal associated with the higher order dynamics is seen as noise in this procedure. The quality of this approximation is measured by the coherence function, which is the linear correlation between input and output as a function of frequency and has values in the interval [0,1]. Turbulence and measurement errors also produce reductions in coherence. An objective of the computations is to maintain adequate coherence (above .6) at all frequencies in the frequency range of interest, and there are numerous devices aimed at doing this, both in shaping the input control histories appropriately and in the computational procedure.

The CIFER® computational steps in the slung load identification are outlined in figure 6.2. First, the available frequency sweep records are concatenated so as to maximize the information for the flight condition. Second, the single-input-single-output (SISO) Bode plots are computed. The concatenated record is divided into overlapping time intervals or windows for the computations and the final frequency responses are obtained as averages of the results from these windows. The window size is a selectable parameter in the process and it determines the lowest frequency for which the frequency response can be given (1/T Hz, T = window size). Coherence also depends in part on window size, and smaller (larger) windows give better coherence at higher (lower) frequencies. For the flight time identification only one window size was used (20secs) to reduce the computation time. In postflight analysis, the computations can be repeated for multiple window sizes and the results combined to optimize coherence at all frequencies using CIFER®'s COMPOSITE utility.

Third, the effects of off-axis control inputs on the SISO frequency response can be removed by computations based on multiple inputs using CIFER®'s MISOSA utility. However, the effects of small off-axis control activity were found to be small and this step was omitted.

Finally, the handling qualities parameters and stability margins were computed from the Bode plots, and load pendulum roots were determined by fitting a second order pole to the load's frequency response in the neighborhood of the pendulum frequency using CIFER®'s NAVFIT utility. This utility also measures the quality of the fit, and the frequency range over which the fit is made can be adjusted to optimize its quality for the given record.

Figure 6.2 Identification Procedure.

(a) Computational Steps

1. Concatenate Frequency Sweep Records
2. Compute Single-Input-Single-Output Bode Plots
   - select window size(s)
   - compute Fourier integral
   - compute spectral functions
   - compute Bode plots
3. Multi-window optimization (postflight only)
4. Remove effects of correlated secondary control inputs (omitted).
5. Compute stability margins and handling qualities parameters from Bode plots.
6. Compute load pendulum roots by fitting 2nd order pole to load Bode plot.

(b) Flight-Time vs. Postflight Procedure

Flight-Time:

- 50 Hz data rate
- TM data dropouts
- Directional gyro bias correction
- Concatenate 3 records each case
- 1-Window averaging (T = 20 seconds)
- SISO analysis

Postflight:

- 100 Hz data rate
- No data dropouts
- Directional gyro bias and drift corrections
- Concatenate all available records each case
- Optimized multi-window averaging (T = 10, 20, 25, 30, 40 seconds)
- SISO analysis

6.4 Flight Time Identification Computations

The flight time computations used a number of simplifications and was subject to some difficulties which may not occur in postflight computations (fig. 6.2). The data records were decimated to 50 Hz while the postflight work used 100 Hz. This reduced computation time significantly but satisfies the working rule of 16 times frequency out to 3Hz. The telemetered data was occasionally subject to extended dropout owing to antenna shadowing while the data recorded on-board for postflight analysis had almost no data dropouts. Extended dropouts were treated by reorienting the aircraft and repeating the record. CIFER® sees the inevitable data spikes and momentary dropouts as high frequency noise which have no significant effect on the data quality.

The flight time computations used 1-window averaging while postflight work could use 5 window sizes to optimize coherence at all frequencies. The flight time computations also used only 3 concatenated records each case, while postflight computations could concatenate all available records from multiple flights for each case. Last, the analysis was based on on-axis records only, that is, single input/single output. Despite these simplifications, the flight time estimates were close to the best postflight results in all cases.

7. Identification Results

7.1 Handling Qualities

The main results for handling qualities are shown in figure 7.1. First, a comparison of the ballasted CONEX with the helicopter alone for the lateral axis indicates a reduction of handling qualities parameters at all airspeeds. Points move toward the Level 1-2 boundary, losing bandwidth or gaining phase delay with the addition of this load, depending on airspeed.

Hover is the flight condition closest to the boundary. In addition, it is seen that other loads can have more significant losses in handling qualities as shown by the hover results for the 1K plate for longitudinal control, and for the 4K block for lateral control. These points are in the Level 2 region owing mostly to a significant loss of bandwidth from that of the helicopter alone. Thus, the effects of the load on handling qualities appear to be highly variable with ordinary differences among slings and loads, even for a very light load.

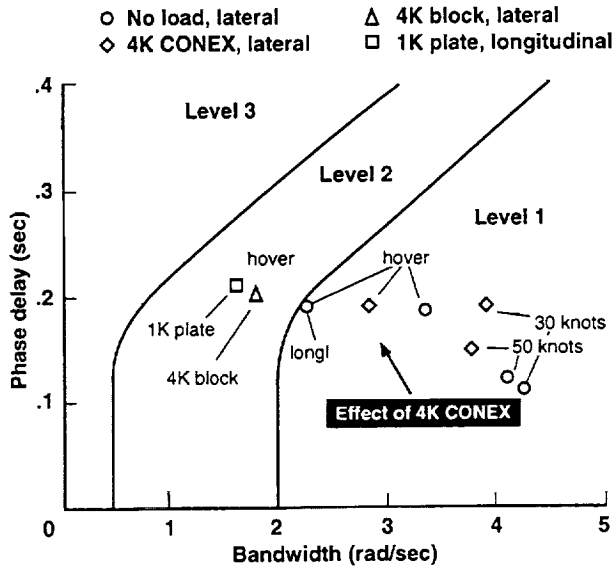

Figure 7.1. Handling qualities parameters.

Handling qualities parameters are plotted vs airspeed in figure 7.2. The lateral axis results repeat those already seen in figure 7.1. For the longitudinal axis, bandwidth is in the range of 2-3 rad/sec in almost all cases, and actually improves somewhat due to the load. An exception is the 1K plate for which bandwidth is reduced below 2rad/sec at hover. Phase delays are between .15 and .2 sec and degraded (increased) by the load in most cases.

The effect of load weight on lateral axis attitude control is shown in figure 7.3, which shows Bode plots for no load, 2K CONEX and 4K CONEX. A gain dip and phase rise occur in the neighborhood of the pendulum frequency due to the dipole-like effect of the load on the helicopter transfer function; and these effects together with a related loss of coherence increase with load weight.

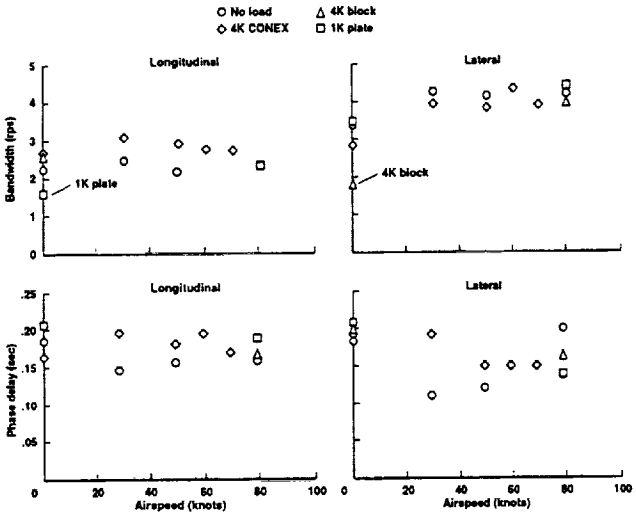

Figure 7.2. Handling qualities vs. Airspeed.

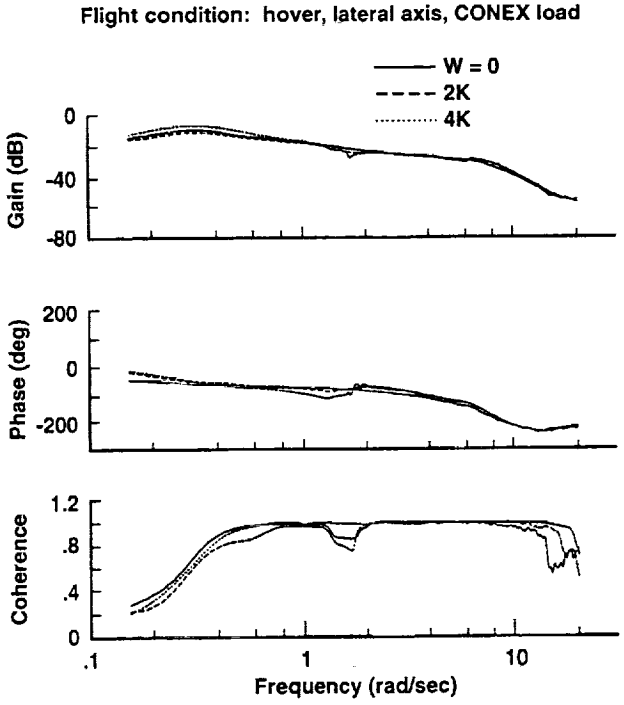

Load weight (lbs)	Bandwidth (rad/sec)	Phase delay (sec)
0	3.33	0.186
2K CONEX	2.87	0.181
4K CONEX	2.82	0.190

Figure 7.3. Effect of load weight on attitude response.

This reflects a loss of helicopter attitude response at the load pendulum frequency as load weight increases. Simulation work at Ames [9] with the CH47 and larger relative load weights than in this study indicates that for sufficiently large weight the bandwidth drops significantly to a value below the pendulum frequency and the pilot then controls the load with much lower frequency inputs. That same work indicates a similar effect of increasing sling length.

7.2 Control System Stability Margins

The principle stability margin results are shown in figure 7.4. A comparison of the lateral axis results for the 4K CONEX with the helicopter alone shows a loss of both gain and phase margin at all airspeeds. Margin losses at hover are 4db and 16 deg for the CONEX, and larger losses occur for the 1K plate and 4K block. The UH-60A is seen to have large margins from the minimums so that moderate losses in margin due to the load don't threaten stability. However, other aircraft can have different base margins and such losses would be more critical. An example is the MH-53J (ref. 22) which is shown in figure 7.4 to have margins near the minimums.

Control system stability margins are plotted vs. airspeed in figure 7.5. Longitudinal axis margins for the 4K CONEX show almost no effect of the load on both margins up to 50kts. There are more significant effects on margins with the block and plate loads for the available comparison points at hover and 80kts. The lateral axis margins indicate a loss in both margins at nearly all airspeeds. This is consistent with industry experience that the lateral axis is the one for which stability is normally degraded by the load (ref. 2).

The effect of load weight on lateral axis control response is seen in figure 7.6. Dips occur in gain and phase owing to the load dipole in the helicopter transfer function, and the effect increases with load weight.

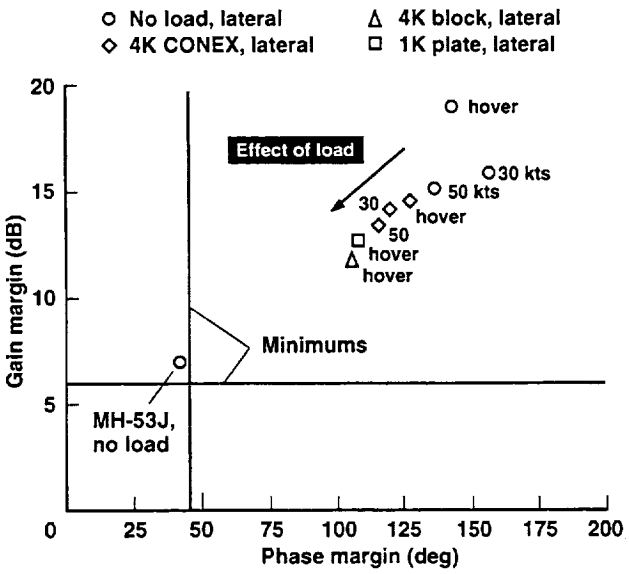

Figure 7.4. Stability margins.

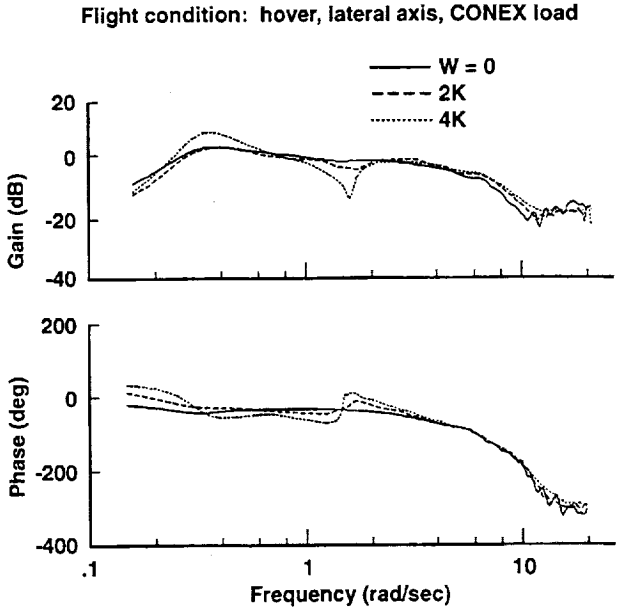

Load weight (lbs)	Gain margin (dB)	Phase margin (deg)
0	19.0	142
2K CONEX	16.5	137
4K CONEX	14.7	126

Figure 7.6. Effect of load weight on control response.

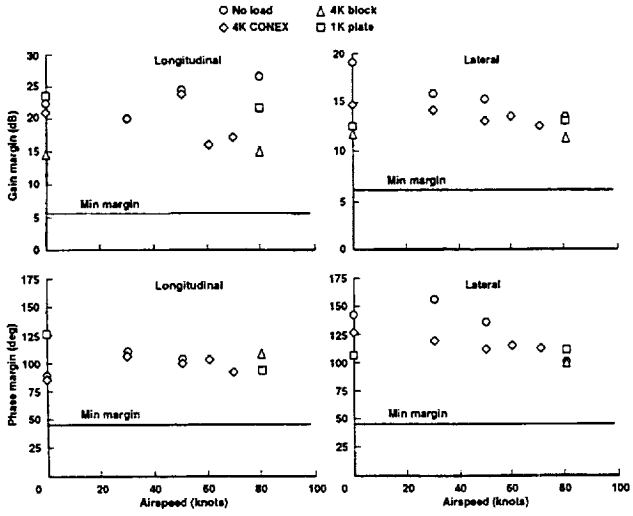

Figure 7.5. Stability margins vs. airspeed.

7.3 Load Pendulum Roots

Damping and natural frequency of the load pendulum modes at hover are shown in figure 7.7, which includes a comparison with simulation results. Frequency is very nearly identical for both modes, around 1.5 rad/sec, and is very well predicted by simulation models. The flight data show moderate damping between .1 and .2 on both axes, while the simulation predicts the longitudinal pendulum to be lightly damped, about 5%, and the lateral pendulum to have twice the measured damping. Thus there is significant disagreement between simulation and flight data on pendulum damping.

Damping and natural frequency are also plotted vs. airspeed in figure 7.7. The pendulum roots are nearly constant with airspeed in these results. Considerable load yaw motion developed with airspeed for the ballasted CONEX but without coupling to the pendulum modes; that is, the load aerodynamics principally influenced the yaw degree of freedom

without modifying the pendulum modes. However, the empty CONEX exhibited considerably more coupling among these degrees of freedom as airspeed increased to 50-60kts, and tests with the empty CONEX at higher speeds might give quite different results.

7.4 Comparison of Flight Time and Postflight Analysis

Adequate coherence was routinely obtained for the helicopter parameter identifications with the flight time procedure. The postflight procedure normally expanded the frequency range with adequate coherence, and increased coherence at most frequencies including at the dipole dip near the pendulum frequency, as seen in the sample case in figure 7.8. These improvements ranged from marginal to significant depending on the case.

For the load response, adequate coherence was difficult to obtain owing to the interference of the load yaw motions in measuring the pendulum swinging motions, the limited range of input frequencies which excite load response, and the suppression of the pendulum mode response to control inputs at higher airspeeds. Identifications were made at hover and 30kts, and these indicated that coherence was marginally acceptable for the longitudinal axis, and much better for the lateral axis.

The flight time procedure provided identifications with adequate coherence for all cases and parameters where this could be done by the postflight procedure.

Improvements of the flight time procedure and system are under consideration. This includes a more efficient user interface, improved computational efficiency and performance, and implementation with a single workstation in conjunction with a portable ground telemetry station.

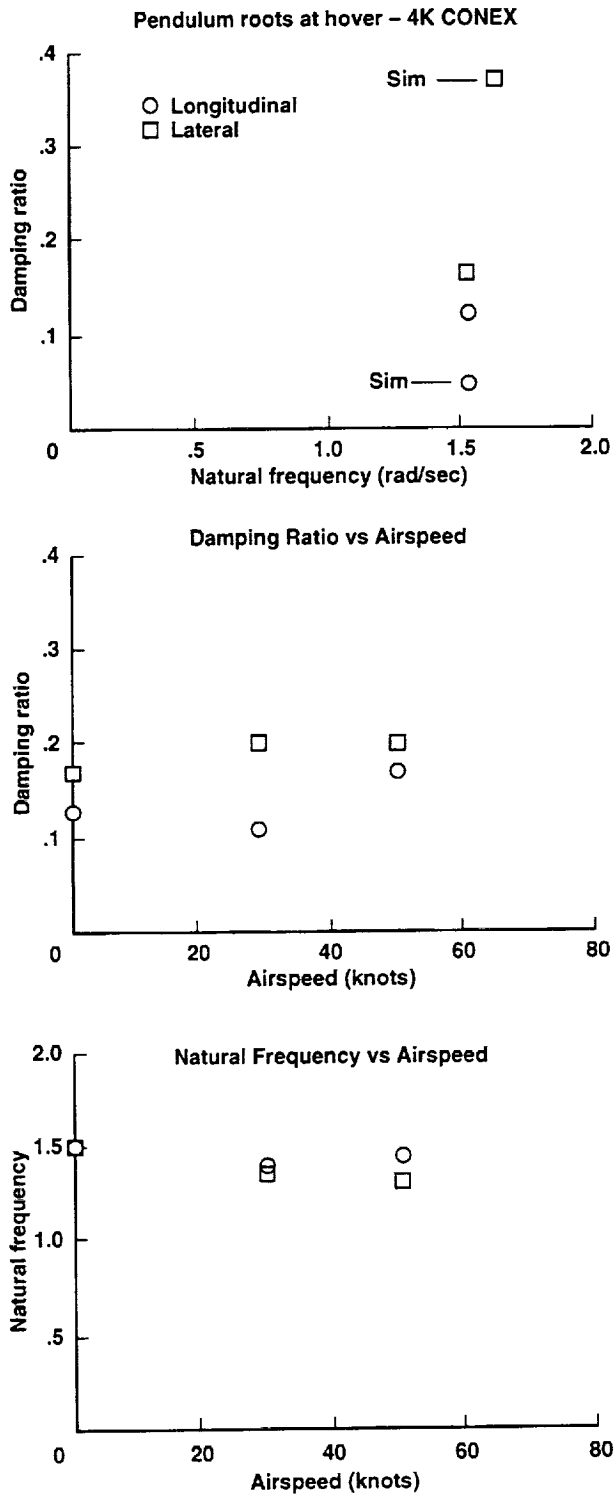

Figure 7.7. Load pendulum modes for 4K lbs. CONEX.

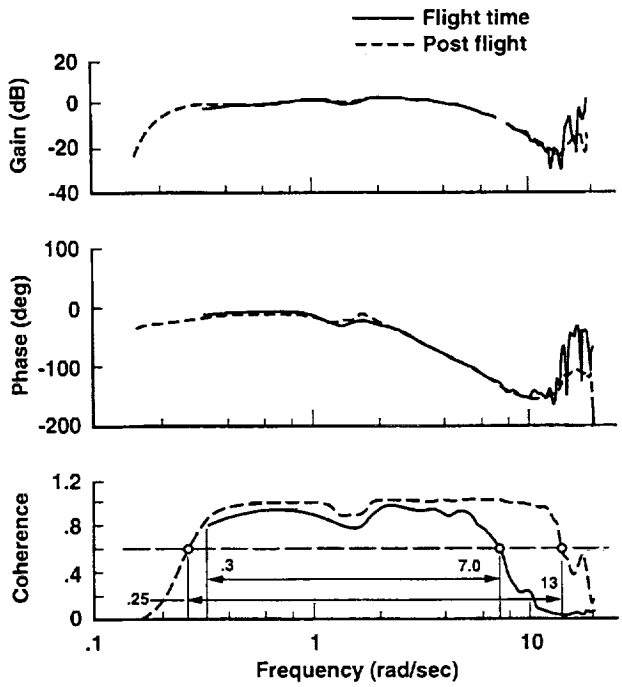

Figure 7.8. Comparison of flight time and post flight analysis. Attitude response, hover, longitudinal axis, 4K CONEX.

8. Simulation of Load Dynamics

8.1 Comparison of Flight and Simulation Load Motions

A simulation model for slung loads is currently under development at Ames. Flight and simulation time histories can be compared by entering the flight test control input histories into the simulation. The simulation contains exact rigid body dynamics for elastic or inelastic slings (ref. 23). The UH-60 aerodynamics are currently represented by a stable linear approximation (ref. 24), and the load aerodynamics are currently limited to drag only.

Results at hover for lateral and longitudinal control frequency sweeps are shown in figures 8.1, and 8.2 for the on-axis angular rates. The sling is modeled as inelastic in the simulation results. The approximate helicopter model is seen to reproduce the helicopter rates fairly well over the test frequency range. The load roll rate history shows good agreement in phase and damping. The load pitch rate history exhibits reasonably good phase agreement but the simulation history shows larger amplitude and longer persistence of the longitudinal pendulum mode than in flight. This is consistent with the difference in damping ratio previously noted for the longitudinal pendulum mode.

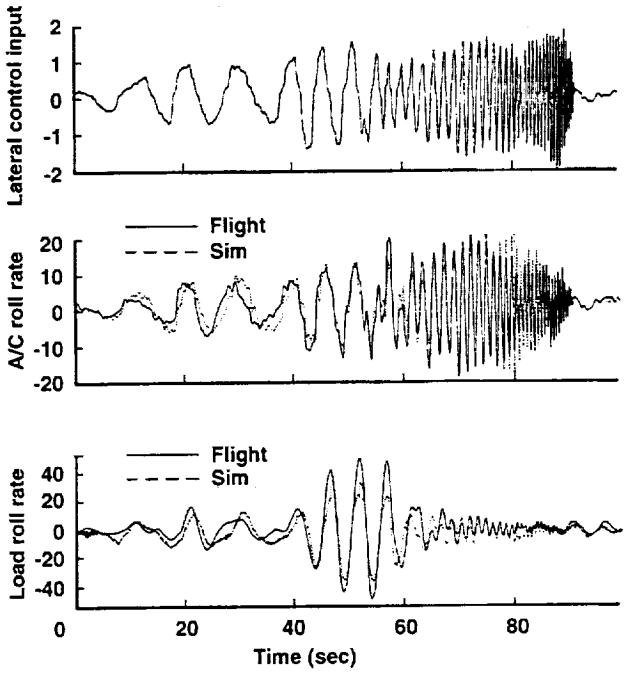

Figure 8.1. Comparison of flight and simulation. Lateral control sweep, hover, 4K CONEX.

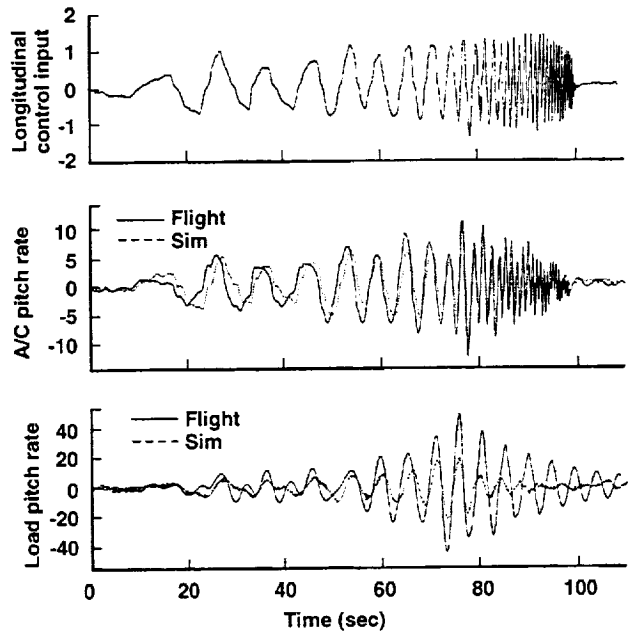

Figure 8.2. Comparison of flight and simulation. Longitudinal control sweep, hover, 4K CONEX.

8.3 Slung Load Simulation Development Issues

Since helicopter model validation has been well advanced in the last decade out to high frequencies (e.g., refs. 2 and 4) the main challenge for validation of a slung load simulation is in modeling the load-sling dynamics. The current flight experience and prior experience with simulations indicate the following points for study and development:

First, there are significant differences in the damping of the pendulum modes between flight and simulation.

Second, the CONEX with swiveled suspension was observed to reach steady yaw rates at hover. This indicates the existence of measurable rotor downwash effects on load motions at/near hover.

Third, load yaw motions differed for swiveled and unswiveled sling. Modeling complexities for the unswiveled sling include sling windup and corresponding variable sling geometry, and yaw resistance moment at the hook.

Fourth, the standard model of the elastic sling as a lightly damped spring which supports only tension was rated by pilots as unrealistic in recent moving based simulation studies at Ames underlying (ref. 9). This model generates significant excursions in hook force when pilot control inputs excite elastic stretching, and corresponding vertical cg motions which were rated unrealistic. Possible causes are unmodeled sling hysteresis, and interactions of sling stretching with the rotor coning dynamics that were not represented in the simulation rotor model.

Last, only limited load aerodynamic data is available. Load aerodynamics can be grouped into static, rotary, and unsteady aerodynamics. The static aerodynamics are, in principle, easiest to measure and model, and are expected to account for the load yaw motions and yaw-pendulum coupling. Prediction of load instability, however, depends on unsteady effects (ref. 26).

A simulation model of the static aerodynamics requires definition of six force and moment components over the complete range of angle of attack [-90,90] and sideslip [-180,180]. Complete coverage is available for the MILVAN (refs. 27 and 28) and the CONEX. Otherwise, the available wind tunnel data is restricted to partial coverage and information. The potential for measuring load aerodynamics from flight test data with an instrumented load remains to be examined.

9. Conclusions

1. A system for computing control system stability and handling qualities parameters for a helicopter and external load during flight testing has been demonstrated. This capability is useful for slung load certification tests owing to the uncertain stability and envelope of the system, and can potentially result in significant reductions in the cost and time.

2. Good agreement was obtained between the simplified flight-time computations and the refined postflight analysis. The flight-time computational procedure achieved sufficient coherence for a reliable identification in all cases where sufficient coherence was obtained by the post-flight procedure.

3. Although the set of load-sling combinations tested at hover was small in number, significant variations in helicopter handling qualities parameters among these combinations were computed. This suggests a large range of effects on stability and handling qualities among common loads and slings.

4. The sensor requirements to identify load pendulum stability were met without difficulty at low airspeeds. However, flight experience indicated yaw rates increase strongly with airspeed to sufficiently high levels that the selected compass and yaw rate sensors did not function adequately above 50kts. Load dynamic range can exceed that of the helicopter in slung load testing and a corresponding sensor dynamic range is required. Additional sensors for load attitude and the hook force vector would allow identification of the load static aerodynamics from flight data.

5. Simulation development issues include significant differences in load pendulum damping from flight values, modeling of rotor downwash effects on load aerodynamics at/near hover, modeling of sling windup and yaw resistance at the hook, sling

stretching dynamics, and limited load aerodynamic data.

11. References

1. Multiservice Helicopter External Air Transport: Vols. I, II, III. US Army FM-55-450-3, 4, 5. Feb. 1991.

2. Lawrence T., Gerdes W., Yakzan S.: Use of Simulation for Qualification of Helicopter External Loads. Proceedings, AHS 50th Annual Forum, May 1994

3. Ten Years of Cooperation on Rotorcraft Aeromechanics and Man-Machine Integration Technology. M. Tischler, A. Kuritsky, editors. Ames Research Center, Oct 1996.

4. Tischler M., Cauffman M.: Frequency-Response Method for Rotorcraft Identification: Flight Applications to BO-105 Coupled Rotor/ Fuselage Dynamics. JAHS, vol. 37, no3, July 1992.

5. Tischler M., Cauffman M.: Comprehensive Identification from Frequency Responses (CIFER®): An Interactive Facility for System Identification and Verification. Vols. 1, 2. NASA Conference Publication 10149, USAATCOM TR-94-A-017. Sept, 1994

6. McCoy A.: Flight Testing and Real Time System Identification Analysis of a UH-60A Black Hawk Helicopter with an Instrumented External Sling Load. NASA CR 1998-196710, April 1998.

7. Handling Qualities Requirements for Military Rotorcraft. US Army Aeronautical Design Standard ADS-33D-PRF. USAATC/AVRDEC, US Army Aviation and Troop Command, St Louis, Mo. May 1996.

8. General Specification for Flight Control Systems: General Specification for Design, Installation, and Test of Piloted Aircraft. MIL-F-9490D. (USAF) June, 1995

9. Key D., Hoh R., Blanken C.: Tailoring ADS-33 for a Specific End Item. 52nd Annual AHS Forum, Wash DC, May 1998.

10. Hilbert K.: Math Model of the UH-60 Helicopter. NASA TM 85890. April 1984.

11. Howlett J.: UH-60A Black Hawk Engineering Simulation Program NASA CR 166309, Dec 1981.

12. Fletcher J.: A Model Structure for Identification of Linear Models of the UH-60 Helicopter in Hover and Forward Flight. NASA TM 110362, Aug 1995.

13. Operator's Manual for Army Models UH-60A, UH-60L, EH-60A Helicopters. Army technical manual TM-1-1520-237-10, 31 Aug 1994

14. Kufeld R., Balough D., Cross J., Studebaker K., Jennison C.,Bousman W.: Flight Testing the UH-60A Airloads Aircraft. AHS Forum Washington DC, May 1994.

15. Black Hawk Slung Load Instrumentation Package: Development Report and User Manual. IAF Flight Test Center, Instrumentation Dept Report for the MOA. Oct 1996

16. Owner's Manual, C100 Electronic Compass. KVH Industries Inc, Middletown, Rhode Island.

17. Owner's Manual, E-79 Electronic Load Weigh System. Onboard Systems, Portland, Oregon, May 1996

18. Tischler M., Fletcher J., Diekman J., Williams V., Cason R.: Demonstration of Frequency Sweep Test Techniques Using a Bell-214-T Helicopter. NASA TM-89422, Apr 1987.

19. Willams J., Ham J., Tischler M., Flight Test Manual: Rotorcraft Frequency Domain Flight Testing. AQTD Project 93-14, US Army Aviation Technical Test Center. Sept 1995.

20. Wei M., Ng S.Y., Somes A., Aoyagi M., Leung J.: Real-Time Server-Client System for the Near Real-Time Research Analysis of Ensemble Data. Paper to be given at International Telemetry Conference, San Diego, Oct 98.

21. Lisoski D., Tischler M.: Solar Powered Stratospheric Research Aircraft Flight Test and System Identification. RTA Symposium on System Identification for Integrated Aircraft Development and Flight Testing. Paper #27, May 1998, Madrid

22. MH-53J AFCS Evaluation. Project A-8867 Final report. Georgia Tech Research Institute, Nov 1993 (for Warner Robins Air Logistics Center, Robins AF Base, Ga. Contract F09603-89-G-00077-0008).

23. Cicolani L., Kanning G., Synnestvedt R.: Simulation of the Dynamics of Slung Load Systems. Journal of the American Helicopter Society, Oct 1995.

24. Whalley M., Carpenter W.: A Piloted Simulation Investigation of Forward Flight Handling Qualities Requirements for Air-to-Air Combat. NASA TM 103919, May 1992.

26. Simpson A., Flower J.: Unsteady Aerodynamics of Oscillating Containers and Application to the Problem of Dynamic Stability of Helicopter Underslung Loads. AGARD CP-235, May 1978.

27. Laub G., Kodani H.: Wind Tunnel Investigation of Aerodynamic Characteristics of Scale Models of Three Rectangular Shaped Cargo Containers. NASA TM X-62169, July 1972

28. Cicolani L., Kanning G.: A Comprehensive Estimate of the Static Aerodynamic Forces and Moments of the 8x8x20 ft Cargo Container. NASA TM 89433. May 1987.

REPORT DOCUMENTATION PAGE

Form Approved
OMB No. 0704-0188

1. AGENCY USE ONLY *(Leave blank)*	2. REPORT DATE	3. REPORT TYPE AND DATES COVERED
	April 1998	Technical Memorandum

4. TITLE AND SUBTITLE

Flight-Time Identification of a UH-60A Helicopter and Slung Load

5. FUNDING NUMBERS

581-30-22

6. AUTHOR(S)

Luigi S. Cicolani, Allen H. McCoy, Mark B. Tischler, George E. Tucker, Pinhas Gatenio, and Dani Marmar

7. PERFORMING ORGANIZATION NAME(S) AND ADDRESS(ES)

Aeroflightdynamics Directorate, U.S. Army Aviation and Troop Command, Ames Research Center, Moffett Field, CA 94035-1000

8. PERFORMING ORGANIZATION REPORT NUMBER

A-9810861

9. SPONSORING/MONITORING AGENCY NAME(S) AND ADDRESS(ES)

National Aeronautics and Space Administration
Washington, DC 20546-0001 and U.S. Army Aviation and Troop Command, St. Louis, MO 63120-1798

10. SPONSORING/MONITORING AGENCY REPORT NUMBER

NASA TM–1998-112231
USAATCOM TR-98-A-004

11. SUPPLEMENTARY NOTES

Point of Contact: Luigi S. Cicolani, Ames Research Center, MS 211-2, Moffett Field, CA 94035-1000
(650) 604-5446

12a. DISTRIBUTION/AVAILABILITY STATEMENT

Unclassified-Unlimited

Subject Category – 08

Available from the NASA Center for AeroSpace Information,
800 Elkridge Landing Road, Linthicum Heights, MD 21090; (301) 621-0390

12b. DISTRIBUTION CODE

13. ABSTRACT ***(Maximum 200 words)***

This paper describes a flight test demonstration of a system for identification of the stability and handling qualities parameters of a helicopter-slung load configuration simultaneously with flight testing, and the results obtained. Tests were conducted with a UH-60A Black Hawk at speeds from hover to 80kts. The principal test load was an instrumented 8x6x6ft cargo container. The identification used frequency domain analysis in the frequency range to 2Hz, and focussed on the longitudinal and lateral control axes since these are the axes most affected by the load pendulum modes in the frequency range of interest for handling qualities. Results were computed for stability margins, handling qualities parameters and load pendulum stability. The computations took an average of 4 minutes before clearing the aircraft to the next test point. Important reductions in handling qualities were computed in some cases, depending on control axis and load-sling combination. A database, including load dynamics measurements, was accumulated for subsequent simulation development and validation.

14. SUBJECT TERMS

Helicopter, External/sling loads, Flight testing, CIFER identification, Helicopter handling qualities, Helicopter stability margins

15. NUMBER OF PAGES

26

16. PRICE CODE

A03

17. SECURITY CLASSIFICATION OF REPORT	18. SECURITY CLASSIFICATION OF THIS PAGE	19. SECURITY CLASSIFICATION OF ABSTRACT	20. LIMITATION OF ABSTRACT
Unclassified	Unclassified		